Dynamic Ion Structure Factor of Warm Dense Matter

J. Vorberger,[1] Z. Donko,[2] I. M. Tkachenko,[3] and D. O. Gericke[1]

[1]*Centre for Fusion, Space and Astrophysics, Department of Physics, University of Warwick, Coventry CV4 7AL, United Kingdom*
[2]*Institute for Solid State Physics and Optics, Wigner Research Centre for Physics, H-1525 Budapest, Hungary*
[3]*Instituto de Matemática Pura y Aplicada, Universidad Politécnica de Valencia, 46022 Valencia, Spain*

(Received 20 August 2012; published 28 November 2012)

The dynamics of the ion structure in warm dense matter is determined by molecular dynamics simulations using an effective ion-ion potential. This potential is obtained from *ab initio* simulations and has a strong short-range repulsion added to a screened Coulomb potential. Models based on static or dynamic local field corrections are found to be insufficient to describe the data. An extended Mermin approach, a hydrodynamic model, and the method of moments with local constraints are capable of reproducing the numerical results but have rather limited predictive powers as they all need some numerical data as input. The method of moments is found to be the most promising.

DOI: 10.1103/PhysRevLett.109.225001 PACS numbers: 52.27.Gr, 52.65.Yy

The dynamic ion structure factor $S_{ii}(k, \omega)$ (DISF) of dense plasmas and warm dense matter (WDM) is of great importance as it contains the complete information on the ions in these strongly interacting systems and is also influenced by the electron properties. It is closely related to the density response function and, thus, determines many relaxation and transport properties, e.g., stopping power and electron-ion temperature equilibration, and even the equation of state [1–3]. The DISF may also be used for the diagnostics of extreme states of matter like WDM by means of x-ray Thomson scattering [4–9].

Ab initio simulations have been successfully applied to describe the properties of WDM including the equation of state and x-ray scattering cross sections [8–11]. However, the calculation of the DISF would require an unrealistic computational effort when using first principle methods. Thus, most efforts on the DISF were focused on model systems such as the one-component plasma (OCP) model, using bare Coulomb interactions, or the Yukawa model, considering screened Coulomb potentials [12–16]. Both models treat ions with an effective charge state but otherwise neglect the effects of bound electrons. In dense matter, full shells of bound electrons can, however, modify the effective ion-ion interactions and lead to significant changes in the static structure factor [17,18]. Consequently, it can be expected that the simple OCP and Yukawa models yield insufficient information on DISFs for most WDM systems created experimentally.

To study the spectrum of ion acoustic modes in WDM more realistically, we apply a significantly improved ion-ion interaction in molecular dynamics (MD) simulations. This effective potential has been extracted from density functional molecular dynamics simulations considering all electrons [18]. This first principle method fully meets the requirements to model WDM as it considers the quantum behavior of the electrons and strong forces between the ions. The resulting effective ion-ion potential can be described as being of Yukawa type with added short-range repulsion (Yukawa+SRR). It can be reproduced excellently by the following form:

$$V_{ii}^{\mathrm{eff}}(r) = \left[\frac{Z_1^2 e^2}{r} + \frac{(Z_c^2 - Z_1^2)e^2}{r} e^{-br}\right] e^{-\kappa r}. \qquad (1)$$

Z_1 is the charge state of the ion and Z_c its nuclear charge. The parameter b determines the onset of the strong short-range repulsion. For large distances, Eq. (1) coincides with the Yukawa potential (first term) but it is much more repulsive for close encounters. In contrast to the Yukawa model, the Yukawa + SRR potential (1) yields the *static* ion structure in very good agreement with first principle simulations of WDM [17,18].

In this Letter, we investigate the *dynamic* properties of the ion subsystem based on the effective potential (1) as it captures the complex interactions in WDM. For all examples, we employ the parameters of an experiment with shocked silicon [19]. Thus, we have $Z_1 = 4$, $Z_c = 14$, $n_e = 5.36 \times 10^{23}$ cm^{-3}, and $T = 54540$ K, which results in $\kappa = 1.277 a_B^{-1}$ and $d = (3/4\pi n_i)^{1/3} = 2.291 a_B$ for the inverse screening length and the interparticle distance, respectively. a_B is the Bohr radius. The classical coupling parameter for these parameters is $\Gamma = 40.4$. Fitting the effective potential (1) to results from the density functional theory yields $b = 0.7 a_B^{-1}$ for the switching parameter.

In our MD simulations, we follow the dynamics of the ions by integrating their equations of motion (using a velocity-Verlet integrator) while accounting for the pairwise interaction of the particles. The relatively strong screening allows us to use a cutoff radius ($R_c = 5.12d$) and to limit the summation of interparticle forces to neighbors within a sphere having a radius R_c where efficient finding of these neighbors is aided by the chaining mesh technique. Our simulations use $N = 4000$ particles and a cubic simulation box with periodic boundary conditions. The dynamic structure factor is calculated for a series

of wave numbers that are multiples of $(kd)_{\min} = 0.2455$. We have carried out 30 simulation runs, each comprising 2^{21} time steps, and average the data obtained from these data sets.

Figure 1 shows our results for the DISF applying the effective ion-ion potential (1) and compares these data to the DISF for a Yukawa system. Because of the modified interactions, the ion acoustic peaks are upshifted, which marks the difference in sound speed. In addition, the height and width of the ion acoustic peaks are changed dramatically and the diffusive peak at $\omega = 0$ is strongly reduced. These differences show that partial ionization in WDM, modeled by the potential (1), can significantly change the ion dynamics.

To gain additional insights into the ion dynamics, we test a number of analytical models against the MD data. First we consider local field corrections (LFC) that are based on the static ion structure. Then, we employ methods with one or more free parameters that allow us to fit the numerical data.

Local field corrections are introduced by connecting the DISF and the ion density response function [3]

$$S_{ii}(k, \omega) = -\frac{k_B T}{\pi\omega} \operatorname{Im}\chi_{ii}(k, \omega), \tag{2}$$

where the latter is expressed as [20]

$$\chi_{ii}(k, \omega) = \frac{\chi_i^0(k\omega)}{1 - V_{ii}^{\text{eff}}(k)[1 - G_{ii}(k, \omega)]\chi_i^0(k\omega)}. \tag{3}$$

Here, $\chi_i^0(k, \omega)$ is the ideal gas response and $G_{ii}(k, \omega)$ is the, generally dynamic, local field correction.

We apply two models for static local field corrections. The first uses the spectral representation of the density response function in the limit $\omega \to 0$ [3]

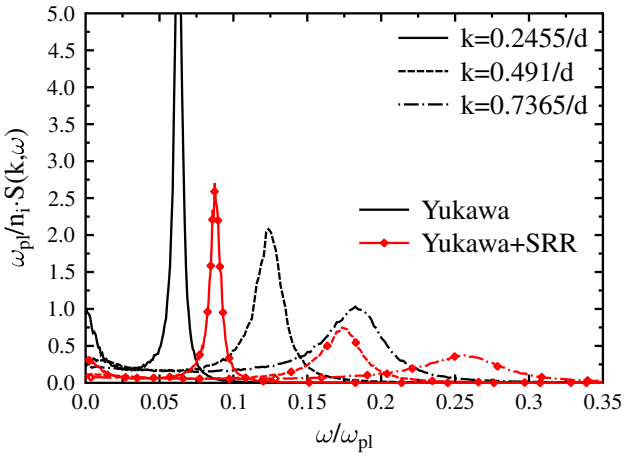

FIG. 1 (color online). DISF for the effective ion-ion potential (1) compared to the one for a Yukawa system. Both results are obtained by MD for the example of shocked silicon [19].

$$G_{ii}(k, 0) = 1 - \frac{k_B T}{n_i V_{ii}^{\text{eff}}(k)}\left[\frac{1}{S_{ii}(k)} - 1\right]. \tag{4}$$

Similarly, the sum rule of the third frequency moment can be exploited in the high frequency limit [21]. For the potential (1) considered here, one obtains

$$G_{ii}(k, \infty) = \frac{4\pi Z_1^2 e^2}{n_i k^2 V_{ii}^{\text{eff}}(k)}[I_1(k, \kappa_1) + \Theta I_c(k, \kappa_c)] \tag{5}$$

with $\Theta = (Z_c^2/Z_1^2) - 1$ and

$$I_a(k, \kappa_a) = \frac{1}{4\pi^2}\int dq q^2[1 - S_{ii}(q)]\left[\frac{3}{2} - \frac{2}{3}\frac{q^2}{q^2 + \kappa_a^2} - \frac{q^2 + \kappa_a^2}{2k^2} + \frac{(q^2 + \kappa_a^2 - k^2)^2}{8qk^3} \times \ln\frac{(q + k)^2 + \kappa_a^2}{(q - k)^2 + \kappa_a^2}\right]. \tag{6}$$

Here, $a = \{1, c\}$, $\kappa_1 = \kappa$ is the normal screening length depending on the electron properties and $\kappa_c = \kappa + b$.

Dynamic local field corrections can be derived using the method of recurrence relations [22,23]. The result is a smooth interpolation between the two static local field corrections at $\omega = 0$ and $\omega = \infty$ presented above

$$G_{ii}(k, \omega) = G_{ii}(k, 0) + \eta_2 Q(k, \omega), \tag{7}$$

$$\eta_2 = -\frac{1}{2}[G_{ii}(k, 0) - G_{ii}(k, \infty)], \tag{8}$$

$$Q(k, \omega) = \frac{\chi_i^0(k, 0)}{\chi_i^0(k, \omega)} + \frac{\omega^2}{\Delta_1^0} - 1. \tag{9}$$

The function $Q(k, \omega)$ switches between the two limiting static LFCs where we defined $\Delta_1^0 = k^2 k_B T/m_i$.

Figure 2 shows that all LFC methods reproduce the numerical DISF very poorly. Neither location, height, width, nor the diffusive peak agree with the MD data for this moderately coupled system. Further analysis of this fact is presented in Fig. 3. Here, the dispersion relation and the width (full width at half maximum—FWHM) of the ion acoustic peak is shown over a range of wave vectors. The static LFC ($\omega = 0$) reproduces the location of the ion acoustic mode reasonably well, but the FWHM is almost an order of magnitude too small. Therefore, one has to acknowledge the failure of LFC methods to reproduce the dynamic ion structure in WDM for arbitrary parameters of coupling and wave vectors.

To overcome these shortcomings of the LFC methods, we follow three alternative approaches:

(1) Recently the *extended Mermin approach* was introduced by Fortmann *et al.* It combines the Mermin ansatz for the dielectric function with the formalism of LFCs to describe both strong correlations and collisions [24]. For the density response function follows

$$\chi_{ii}^{\mathrm{exM}}(k,\omega)=\left[1-\frac{i\omega}{\nu(\omega)}\right]\left\{\frac{\chi_{ii}^{\mathrm{LFC}}[k,\omega+i\nu(\omega)]\chi_{ii}^{\mathrm{LFC}}(k,0)}{\chi_{ii}^{\mathrm{LFC}}[k,\omega+i\nu(\omega)]-[i\omega/\nu(\omega)]\chi_{ii}^{\mathrm{LFC}}(k,0)}\right\}. \quad (10)$$

$\chi_{ii}^{\mathrm{LFC}}(k,\omega)$ contain LFCs as in Eq. (3) and the collision frequency $\nu(\omega)$ can be calculated, e.g., in the Born approximation [24,25]. However, this approach is usually used for systems with Coulomb interactions. In our case, the effective ion-ion potential introduces some of the physics usually included in the dynamic collision frequency. The collision frequency here describes ion-ion and electron-ion correlations beyond the ion LFCs used earlier. An identification in terms of the usual Born or T-matrix electron-ion collision frequencies seems difficult if not impossible. For this reason, we have chosen to use the static collision frequency ν as an adjustment parameter. Moreover, it is found that collision frequencies with identical real and imaginary parts give the best agreement with the MD data for most cases in this paper.

(2) Within the *method of moments with local constraints*, the density response function is expanded in the space of frequency moments $S_\mu(k)=n_i^{-1}\int_{-\infty}^{+\infty}d\omega\omega^\mu S_{ii}(k,\omega)$ [26,27]. This method has the large advantage that an arbitrary number of sum rules for the response function is satisfied exactly. For the DISF, we have

$$\frac{\pi}{n_i}S_{ii}(k,\omega)=\frac{S_{ii}(k)\omega_1^2\Delta_2\mathrm{Im}\zeta(k,\omega)}{[\omega\Delta_2+\Delta_1\mathrm{Re}\zeta(k,\omega)]^2+[\Delta_1\mathrm{Im}\zeta(k,\omega)]^2} \quad (11)$$

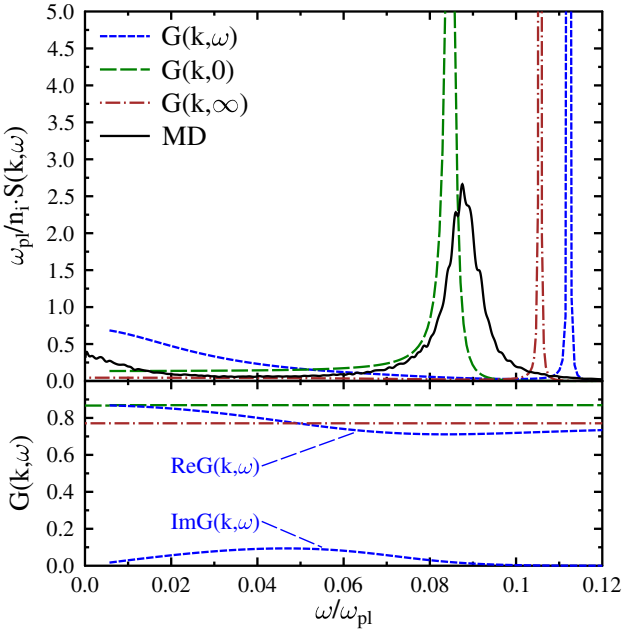

FIG. 2 (color online). DISF obtained with MD simulations and from theories applying different LFCs for the effective potential (1) and a wave number $kd=0.2455$. Bottom panel: LFC entering the calculations for the respective DISF.

with $\Delta_j=\omega^2-\omega_j^2$. The characteristic frequencies ω_j are defined by the moments of the DISF: $\omega_1^2=S_2(k)/S_0(k)$ and $\omega_2^2=S_4(k)/S_2(k)$. The zeroth moment is the static structure factor $S_0(k)=S_{ii}(k)$, the second moment is the f-sum rule, and the fourth moment is related to $G(k,\infty)$

$$\omega_2^2=\frac{n_i}{m_i}\left\{\frac{3k^2k_BT}{n_i}+k^2V_{ii}^{\mathrm{eff}}(k)[1-G_{ii}(k,\infty)]\right\}. \quad (12)$$

The Nevanlinna function $\zeta(k,\omega)$ contains all higher order correlations and can be related to the dynamic LFC of Eq. (7) [26]. This function, chosen from a certain mathematical class, does not influence the fulfilment of the sum rules. In the simplest approximation, the Nevanlinna function is purely imaginary and static

$$\zeta(k)=\frac{i}{\tau}=i\frac{n_iS_{ii}(k)\omega_{pl}^2\Delta'(k)}{\pi S_{ii}(k,0)\omega_1^2}. \quad (13)$$

Here, $\Delta'(k)=(\omega_2^2-\omega_1^2)/\omega_{pl}^2$ with the plasma frequency $\omega_{pl}^2=4\pi Z_1^2e^2n_i/m_i$. A better approximation for $\zeta(k,\omega)$ can be obtained via the Schur algorithm within the Nevanlinna pick problem involving a Hilbert transform of the DISF at one or more points in an optimization procedure [26,27]. This formalism also creates a real part of the Nevanlinna function $\zeta(k)=\mathrm{Re}\zeta(k)+i\mathrm{Im}\zeta(k)$. For our purpose of reproducing the numerical data for the DISF, we find that a one-point constraint, carefully chosen from the set of MD data, is sufficient.

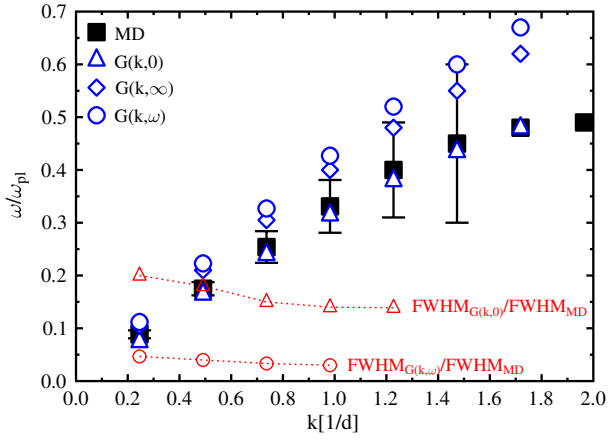

FIG. 3 (color online). Dispersion relation of the ion acoustic mode obtained from MD and different LFC theories applying the potential (1). The FWHM of the ion acoustic peaks are indicated by error bars for the MD data. The ratio of FWHMs from LFC and MD are given separately.

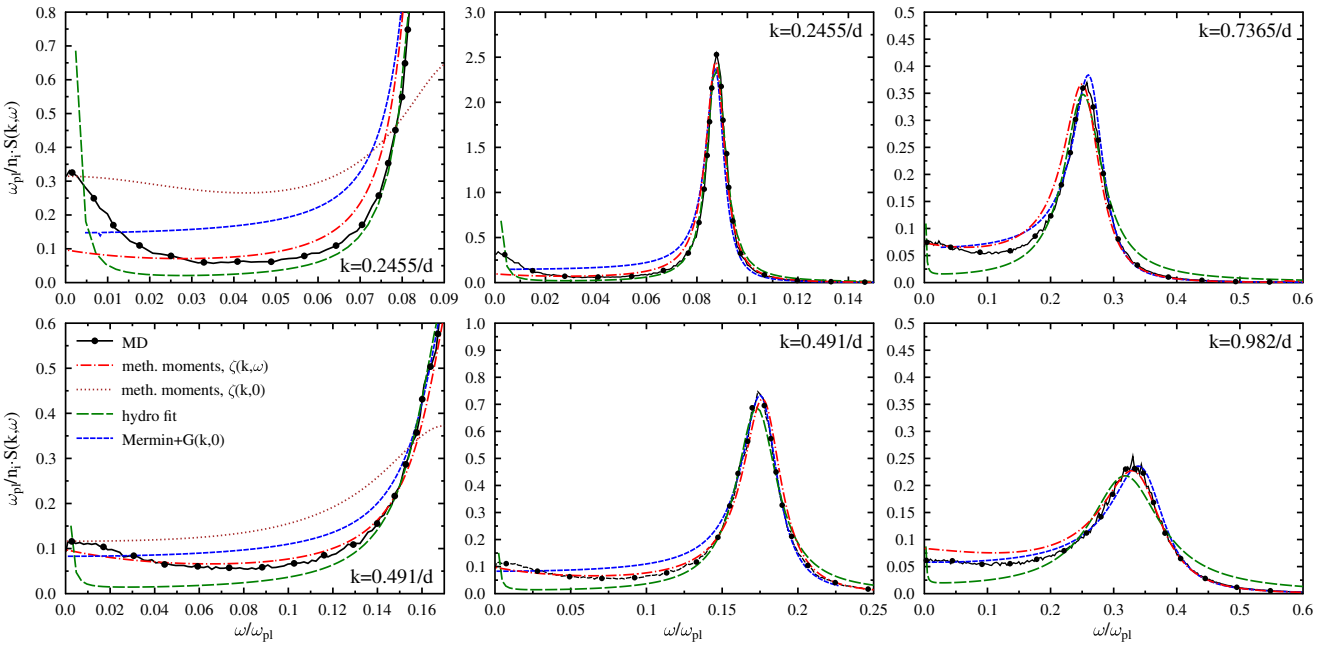

FIG. 4 (color online). DISF of the Yukawa + SRR system for four different wave vectors in different approximations: MD (black line with dots), Mermin $+G(k, 0)$ (blue, short dashed line), hydrodynamic model (green, long dashed line), method of moments with one local constraint (red, dash-dotted line), and method of moments with the static Nevanlinna function (brown, dotted line).

(3) The *hydrodynamic model* was used quite successfully to reproduce the DISF for OCP and Yukawa systems [16,28]. Within this approach, the DISF is expressed in terms of the static structure $S_{ii}(k)$, the sound speed c_s, the thermal diffusivity D_T, the sound attenuation coefficient σ, and the ratio of specific heats γ

$$\frac{S_{ii}(k,\omega)}{S_{ii}(k)} = \frac{\gamma-1}{\gamma}\frac{2D_T k^2}{\omega^2+(D_T k^2)^2} + \frac{1}{\gamma}\left[\frac{\sigma k^2}{(\omega+c_s k)^2+\sigma^2 k^4} + \frac{\sigma k^2}{(\omega-c_s k)^2+\sigma^2 k^4}\right]. \quad (14)$$

Using all of these methods, extended Mermin, method of moments with local constraints, and the hydrodynamic fit, it is possible to obtain a reasonable agreement with the MD data, both for the dispersion relation *and* the actual spectral form of the ion acoustic peak (see Fig. 4). Of course, this success comes at the price of introducing free fit parameters. In case of the hydrodynamic model, there are four independent parameters and the extended Mermin approach uses two: the real and imaginary parts of the collision frequency. The method of moments can reproduce the MD data very well by using just one local constraint, that is, a point chosen from the MD data. As the hydrodynamic model is strictly valid for small wave vectors only and the collision frequency, used here as a fit parameter, lacks physical meaning, the method of moments is our preferred model.

As shown in Fig. 4, the ion acoustic mode is reproduced well by the three methods above. However, there is a consistent problem of all tested methods to describe the diffusive peak near $\omega = 0$ correctly. To determine whether this discrepancy was due to numerical bias, we evaluated the static structure factor, the f-sum rule, and the fourth moment of the DISF from MD simulations and the analytical approaches. For all wave vectors analyzed here, we found less than 1% and less than 5% deviations for the f-sum rule and the fourth moment sum rule, respectively. All static properties entering the analytic models are thus highly accurate, making the failure to describe the diffusive peak even more remarkable. However, this deficit is mitigated by the fact that most of the spectral weight is contained in the ion acoustic mode for small wave vectors. Thus, the diffusive mode constitutes only a small contribution to the ion dynamics.

In conclusion, we have demonstrated that the complex interactions in WDM significantly modify the dynamics of the ions. Whereas LFC cannot reproduce the DISF from MD simulations, theories with few free parameters are sufficient. Overall, we prefer the method of moments to describe the DISF. It is not restricted to small wave vectors and conserves all known exact sum rules.

J. V. thanks the Technische Universität Kaiserslautern (Germany) for its generous hospitality. I. M. T. is grateful to the UPV for the sabbatical leave he was granted. J. V. and D. O. G. acknowledge support from EPSRC

(Grant No. EP/I014888/1) and Z. D. acknowledges support from OTKA, Grants No. K77653, No. IN85261, and No. K105476. I. M. T. was partially supported by the Spanish Ministerio de Ciencia e Innovación under Grant No. ENE2010-21116-C02-02.

[1] D. O. Gericke and M. Schlanges, Phys. Rev. E **60**, 904 (1999).
[2] J. Vorberger, D. O. Gericke, Th. Bornath, and M. Schlanges, Phys. Rev. E **81**, 046404 (2010).
[3] D. Kremp *et al.*, *Quantum Statistics of Nonideal Plasmas* (Springer-Verlag, Berlin, Heidelberg, 2005).
[4] A. L. Kritcher *et al.*, Phys. Rev. Lett. **103**, 245004 (2009).
[5] B. Barbrel *et al.*, Phys. Rev. Lett. **102**, 165004 (2009).
[6] S. H. Glenzer and R. Redmer, Rev. Mod. Phys. **81**, 1625 (2009).
[7] J. Gregori and D. O. Gericke, Phys. Plasmas **16**, 056306 (2009).
[8] E. G. Saiz *et al.*, Nat. Phys. **4**, 940 (2008).
[9] A. Pelka *et al.*, Phys. Rev. Lett. **105**, 265701 (2010).
[10] J. Vorberger, I. Tamblyn, B. Militzer, and S. Bonev, Phys. Rev. B **75**, 024206 (2007).
[11] B. Holst, R. Redmer, and M. P. Desjarlais, Phys. Rev. B **77**, 184201 (2008).
[12] J. P. Hansen, E. Pollock, and I. McDonald, Phys. Rev. Lett. **32**, 277 (1974).
[13] F. Nardin, G. Jacucci, and M. Dharma-wardana, Phys. Rev. A **37**, 1025 (1988).
[14] Z. Donko, G. Kalman, and K. Golden, Phys. Rev. Lett. **88**, 225001 (2002).
[15] G. J. Kalman, Z. Donkó, P. Hartmann, and K. Golden, Phys. Rev. Lett. **107**, 175003 (2011).
[16] J. P. Mithen, J. Daligault, and G. Gregori, Phys. Rev. E **83**, 015401(R) (2011).
[17] K. Wünsch, J. Vorberger, and D. O. Gericke, Phys. Rev. E **79**, 010201(R) (2009).
[18] J. Vorberger and D. O. Gericke (to be published).
[19] A. Ng, P. Celliers, G. Xu, and A. Forsman, Phys. Rev. E **52**, 4299 (1995).
[20] G. D. Mahan, *Many Particle Physics* (Plenum Press, New York, 1990).
[21] N. Iwamoto, Phys. Rev. A **30**, 3289 (1984).
[22] J. Hong and M. H. Lee, Phys. Rev. Lett. **55**, 2375 (1985).
[23] J. Hong and C. Kim, Phys. Rev. A **43**, 1965 (1991).
[24] C. Fortmann, A. Wierling, and G. Röpke, Phys. Rev. E **81**, 026405 (2010).
[25] H. Reinholz, R. Redmer, G. Röpke, and A. Wierling, Phys. Rev. E **62**, 5648 (2000).
[26] Y. V. Arkhipov, A. Askaruly, D. Ballester, A. E. Davletov, I. M. Tkachenko, and G. Zwicknagel, Phys. Rev. E **81**, 026402 (2010).
[27] Y. V. Arkhipov, A. Askaruly, A. E. Davletov, and I. M. Tkachenko, Contrib. Plasma Phys. **50**, 69 (2010).
[28] J. P. Mithen, J. Daligault, and G. Gregori, Phys. Rev. E **85**, 056407 (2012).